Teboroxime, Sestamibi and Thallium-201 as Markers of Myocardial Hypoperfusion: Comparison by Quantitative Dual-Isotope Autoradiography in Rabbits

Howard Weinstein, Christopher P. Reinhardt and Jeffrey A. Leppo

Departments of Nuclear Medicine and Medicine (Cardiovascular Division), Myocardial Isotope Research Lab, University of Massachusetts Medical Center, Worcester, Massachusetts

The scintigraphic assessment of myocardial hypoperfusion depends on the ability of imaging agents to delineate flow disparities. Accordingly, we compared the differential uptake of teboroxime, sestamibi and ^{201}Tl in normal and hypoperfused myocardium using quantitative dual isotope autoradiography. Rabbits with acute coronary occlusions (n = 29) received dual isotope injections of teboroxime ^{201}Tl or sestamibi ^{201}Tl or single isotope tracer injections. A group of sham-operated controls (n = 15) received teboroxime and/or ^{201}Tl. Multiple 30-μ short axis slices were collected from each heart and mounted on x-ray film along with tissue standards to independently generate separate ^{99m}Tc and ^{201}Tl autoradiographs. Teboroxime and sestamibi produced greater normal-to-defect activity contrast than ^{201}Tl in each dual isotope heart (range 8.4–48.9 [teboroxime] versus 2.6–12.3 [^{201}Tl], $p < 0.02$ and 4.5–10.4 [sestamibi] versus 3.6–7.3 [^{201}Tl], $p < 0.03$). Similar profiles were obtained in the single isotope hearts. Teboroxime produced larger autoradiographic defects than ^{201}Tl in the dual-isotope hearts [16.0% ± 5.6% (teboroxime) versus 12.9% ± 5.3% (^{201}Tl) of the LV, $p < 0.02$]. We conclude that the ^{99m}Tc-based perfusion agents teboroxime and, to a lesser extent, sestamibi, delineate hypoperfused myocardium more clearly than ^{201}Tl. Teboroxime detects the largest area of hypoperfusion and may provide the most accurate assessment of myocardium at risk.

J Nucl Med 1993; 34:1510–1517

The scintigraphic evaluation of coronary blood flow in the setting of thrombolysis and revascularization for acute ischemic syndromes depends on imaging agents that can accurately determine the presence and extent of myocardium at risk. Although the myocardial kinetics of sestamibi and teboroxime differ from each other and from ^{201}Tl (*1–7*), all three agents are used to evaluate coronary artery disease. Clinical and experimental studies have found that teboroxime and sestamibi can detect myocardial regions distal to acute coronary occlusions (*8–11*). However, no prior study has compared the myocardial uptake of all three agents in a standard model of acute coronary hypoperfusion, nor have previous comparisons used a quantitative high resolution imaging system.

The issue of imaging resolution is important because diagnostic accuracy of teboroxime, sestamibi and ^{201}Tl depends on the ability of these agents to differentiate disparities of regional myocardial blood flow. However, the ability to evaluate tracer uptake by clinical imaging is limited by photon scatter, attenuation and background activity, as well as an inherent difference in Anger camera sensitivity for ^{99m}Tc and ^{201}Tl. In contrast, basic experimental models of tracer uptake achieve excellent counting statistics for ^{99m}Tc and ^{201}Tl but are limited by an arbitrary selection of discrete myocardial segments to determine regional distribution patterns (*4,6,7,12–16*). All of these clinical and basic methods are limited in the resolution attainable and, at best, can only abstractly define border zones. Evaluation of tracer uptake by autoradiography can produce high resolution images (*17–22*) and can accomplish the quantitative comparison of two simultaneously injected tracers with appropriate tissue standards.

Accordingly, we assessed the differential uptake of sestamibi, teboroxime and ^{201}Tl in normal, hypoperfused and border-zone rabbit myocardium by quantitative dual-isotope autoradiography.

METHODS

Radiopharmaceuticals

Teboroxime and sestamibi were obtained as lyophilized kits from Squibb Diagnostics (Princeton, NJ) and EL du Pont de Nemours and Co. (Wilmington, DE), respectively. Up to 200 mCi of ^{99m}Tc pertechnetate in 1 ml of saline was added to each vial. The vials were heated in a water bath at 100°C for 15 min (teboroxime) or 10 min (sestamibi), then cooled to room tempera-

Received Dec. 17, 1992; revision accepted Apr. 27, 1993.
For correspondence or reprints contact: Howard Weinstein, MD, Nuclear Medicine, University of Massachusetts Medical Center, 55 Lake Ave. North, Worcester, MA 01606.

TABLE 1
Experimental Protocol

	Dual-isotope	Single-isotope			Dual-isotope
	MIBI/^{201}Tl	MIBI	^{201}Tl	Teboroxime	Teboroxime/^{201}Tl
Occluded (n)	6	6	5	5	7
Control (n)	0	0	5	5	5

ture. Radiochemical purity was confirmed by paper chromatography (teboroxime) or thin layer chromatography (sestamibi) to exceed 90% in all kits.

Experimental Protocol

New Zealand White male rabbits (n = 44, 1.8–3.5 kg, Millbrook Farms, Amherst, MA) were anesthetized with intravenous sodium pentobarbital (30–50 mg/kg) and ventilated with a Harvard Rodent Ventilator through an endotracheal tube. Supplemental oxygen was administered as needed. Local surgical analgesia was achieved with subcutaneous lidocaine. The left ventricle was catheterized via the carotid artery and the left ventricular pressure continuously recorded. The heart was exposed in a pericardial cradle through a left thoracotomy. Rabbits were then divided into occlusion (n = 29) and sham-operated control (n = 15) groups, as shown in Table 1. The control group permitted the evaluation of the global uptake pattern of ^{201}Tl and ^{99m}Tc (teboroxime) in normal myocardium and was not repeated for sestamibi. In the group of 29 occluded hearts, segmental hypoperfusion was produced by ligation of a major branch of the left circumflex artery. Five minutes later, teboroxime or sestamibi (50–80 mCi) and ^{201}Tl (200–300 μCi) were coinjected (to ensure that uptake occurred under identical coronary blood flow) and allowed to circulate for 5 min (sestamibi/^{201}Tl) or 2 min (teboroxime/^{201}Tl). In the group of rabbits receiving dual isotope teboroxime/^{201}Tl injections, circulation time was shortened for both tracers to prevent rapid redistribution of teboroxime (*23*). To ensure that the uptake or the analysis of each isotope was not affected by the presence of the second isotope, three additional groups of rabbits (total n = 15) received only a single injection of one of these three tracers.

Preparation of Autoradiographs

Hearts were excised and washed, the ventricles filled with embedding medium (OCT, Miles Inc., Elkhart, IN) and quick-frozen in liquid nitrogen. Multiple 30-μ short axis slices from each heart were collected on tape (Type 820, 3M, St. Paul, MN) in a cryomicrotome (PMV 2250, LKB Instruments, Gaithersburg, MD), air-dried at room temperature and mounted face-up on cardboard.

For each experiment, tissue standards were prepared for the relevant isotope(s), consisting of 21 tissue paste samples per isotope in exponentially increasing activity concentrations (*24*). Tissue standards were necessary to convert film intensity on the autoradiographs (a hardware-specific measure of film darkening, expressed in arbitrary units) to tracer activity (the accumulated activity, expressed in nCi/hr). The standards were frozen in carboxymethylcellulose (^{201}Tl) or OCT (^{99m}Tc) and 30-μ slices were co-mounted with each set of heart slices. The heart slices, along with their corresponding standards, were placed on single-coated x-ray film (MRM-1, Eastman Kodak, Rochester, NY), vacuum-sealed in black plastic bags to ensure direct apposition to the film and set aside for exposure.

In the dual isotope hearts, the two isotopes were separated based on their different half-lives (6 hr versus 73 hr for ^{99m}Tc and ^{201}Tl, respectively) in the presence of an initial excess of ^{99m}Tc. The first 1–2 hr exposure imaged the ^{99m}Tc. A second 4–7-day exposure, beginning after the ^{99m}Tc had decayed (Day 4), recorded the ^{201}Tl image. No ^{99m}Tc standards were present on the ^{201}Tl images, demonstrating that the ^{201}Tl autoradiographs were free from detectable ^{99m}Tc crossover. Based on the quantitation of the ^{201}Tl standard discs on the ^{99m}Tc films, ^{99m}Tc-to-^{201}Tl crossover was likewise not appreciable ($<5\%$). Single isotope autoradiographs were exposed for ^{99m}Tc (1–2 hr) and ^{201}Tl (4–7 days), as noted above. Films were developed in an automatic x-ray film processor (RP X-OMAT, Eastman Kodak, Rochester, NY).

Analysis of Autoradiographs

Representative autoradiographs from each experiment were digitized on a shielded lightbox with a video camera and dedicated image capture hardware. Intensity images were signal-averaged over 16 passes to reduce noise. A blank image encompassing the same field-of-view as the myocardium was then subtracted from each image to simultaneously compensate for background film intensity and lightbox nonuniformity. Images were then recorded in a 512 × 512 matrix on an Apple personal computer (Macintosh IIfx, Apple Computer, Cupertino, CA). Digitized images were analyzed using appropriate software (Image V.1.41, NIH, public domain).

For hearts in the coronary occlusion group, tangential lines were drawn across the defects midway between the subendocardium and the subepicardium. Each line included normal myocardium on either side of the defect. In the dual-isotope hearts, alignment of the ^{99m}Tc and ^{201}Tl images was ensured by pinhole markers used with the image analysis software. The intensity value of each pixel along these profile lines was then converted to the actual tracer activity at that point, with reference to its corresponding standard curve. This process is described below.

Each activity curve was normalized to the mean activity along the profile line and depicts the uptake of the tracers across a defect in the following sequence: normal tissue, transition zone, defect, transition zone, normal tissue (Fig. 2). Defect contrast was calculated from the activity profiles as the ratio of normal-to-mean defect activities. Defect contrast for teboroxime or sestamibi was compared to its corresponding ^{201}Tl value in each dual-isotope heart. The mean defect contrast of teboroxime, sestamibi and ^{201}Tl were also compared for the single-isotope hearts.

For the dual-isotope hearts, the operator-defined perimeter of defect was circumscribed for the ^{99m}Tc image and independently for its counterpart ^{201}Tl image. Relative defect area (as a percent of the area of the entire left ventricular wall) was compared for the tracers.

Control Measurements

Autoradiographs from the sham-operated control rabbits injected with teboroxime and ^{201}Tl were assessed for uniformity of tracer uptake across multiple profile lines to rule out any systematic gradient in uptake caused by the noncardiac surgical technique.

It was also possible that the quantitative autoradiography technique utilized may have been inherently more sensitive for either ^{201}Tl or ^{99m}Tc. Accordingly, we evaluated profile lines derived from multiple standard discs containing pure ^{201}Tl or pure ^{99m}Tc to determine if these profiles precisely overlapped.

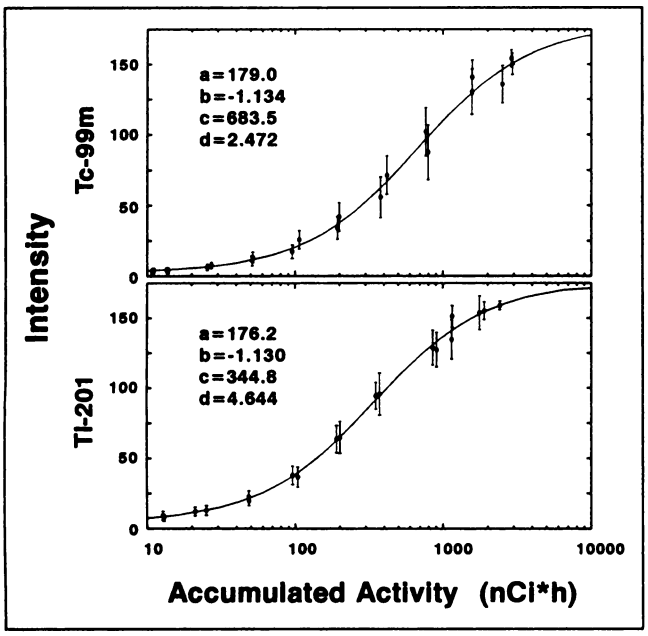

FIGURE 1. Representative standard curves for ^{99m}Tc and ^{201}Tl. For each standard, mean intensity (in arbitrary units ± s.d.) is plotted against accumulated tracer activity. The corresponding sigmoidal curve is shown for each set of standards. Values a, b, c and d represent parameters of sigmoidal function (Equation 2).

Conversion of Intensity to Activity

For each experiment, samples of tissue paste standards were weighed and counted in a NaI (Tl) gamma counter (Auto-Gamma 5530, Packard Instruments, Downers Grove, IL) and decay corrected. The activity concentration of each sample (dpm/mg) was determined based on the counting efficiency of the detector for ^{99m}Tc and ^{201}Tl.

For each set of standard discs, accumulated activity contained in each standard disc was graphed against its average intensity on a semi-log plot. The accumulated activity, $\bar{A}$, contained in a given standard disc during the film exposure was calculated as follows:

$$\bar{A} = Ame^{\lambda t_1} \int_0^{t_2} e^{-\lambda t}\, dt, \qquad \text{Eq. 1}$$

where A is the activity of the standard measured in the gamma counter (dpm/mg); m is the mass of a 30-μ standard disc (0.85 mg); λ is the decay constant of the radioisotope (s^{-1}); t_1 is the interval between the start of exposure and the counting of standards in the gamma counter(s); and t_2 is the duration of exposure(s).

The response of photographic film to radiation exposure is nonlinear, as defined by the H & D curve (*25*). Results of each set of standards were then fit, using the least squares method, to a sigmoidal function, defined by the following equation (Fig. 1):

$$I = \frac{(a - d)}{1 + \left(\frac{\bar{A}}{c}\right)^b} + d, \qquad \text{Eq. 2}$$

where I is the corresponding intensity value; a is a constant which represents the maximum intensity value; b is a constant that describes steepness of the curve; c is a constant that represents accumulated activity value at the inflection point; and d is a constant that represents minimum intensity value.

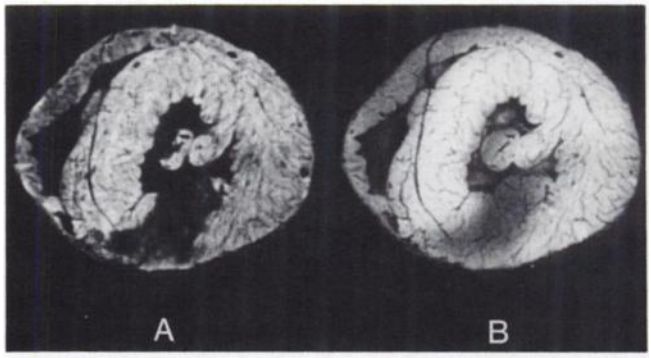

FIGURE 2. Representative pair of digitized dual-isotope activity autoradiographs showing ^{99m}Tc teboroxime (A) and ^{201}Tl (B) activity distributions in the same heart. Note the increased contrast and clearer delineation of normal and low flow zones produced by teboroxime compared to simultaneously injected ^{201}Tl.

Intensity data was thereby converted to accumulated activity using parameters obtained from the above fit. The actual myocardial accumulated activity values spanned the region from ~10–1000 nCi/hr (Fig. 1).

Statistics

Normal-to-defect contrast ratios and defect areas from the dual-isotope hearts were compared using the Wilcoxon Matched-Pairs Signed-Ranks test. Contrast ratios from the single-isotope hearts were compared using Scheffe's test of analysis of variance.

RESULTS

Teboroxime Versus Thallium-201

Teboroxime autoradiographs appeared more sharply defined than their ^{201}Tl counterparts in both dual- and single-isotope experiments. A representative pair of dual-isotope teboroxime and ^{201}Tl activity images from a heart with a coronary occlusion is shown in Figure 2. The uptake profiles across the defects from this pair of dual-isotope images (Fig. 3) showed that the transition zone, from normal-to-low flow zones, was steeper for teboroxime than for ^{201}Tl and was a consistent finding in all hearts. Normal-to-defect contrast ratio was defined as the relative tracer activity in the normal zone divided by that in the low flow zone. The contrast ratio for teboroxime (range 8.4–48.9) exceeded ^{201}Tl (2.6–12.3) in each of the seven dual isotope teboroxime ^{201}Tl hearts, as displayed on the left side of Figure 4. The observed increased contrast of teboroxime relative to ^{201}Tl in the dual-isotope hearts was also noted when comparing contrast values for the single isotope experiments (Table 2).

Hypoperfusion produced by coronary occlusion resulted in larger autoradiographic defects from teboroxime than from simultaneously injected ^{201}Tl (16.0% ± 5.6% of the left ventricle for teboroxime compared to 12.9% ± 5.3% for ^{201}Tl, Table 3).

Sestamibi Versus Thallium-201

Sestamibi autoradiographs appeared more sharply defined than their corresponding ^{201}Tl images. A representative pair of dual-isotope sestamibi and ^{201}Tl activity images from a heart with a coronary occlusion is shown in Figure

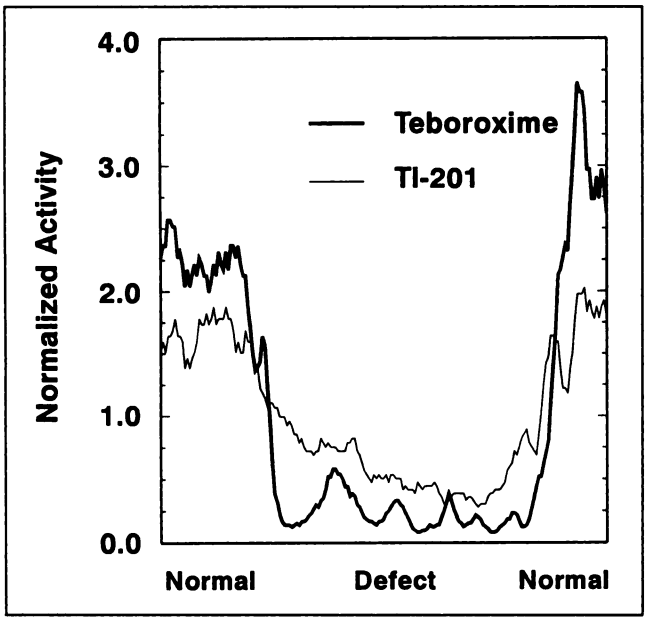

FIGURE 3. Representative pair of dual-isotope ^{99m}Tc teboroxime/^{201}Tl profiles across a defect showing an increased normal-to-defect contrast and a sharper normal-to-defect transition for teboroxime compared to simultaneously injected ^{201}Tl.

5. The apparent difference in contrast for this pair of dual-isotope images, while less than the difference between teboroxime and ^{201}Tl, was confirmed by the uptake profiles (Fig. 6). As displayed in Table 2 and the right side of Figure 4, the normal-to-defect contrast ratio for sestamibi (range 4.5–10.4) was greater than for ^{201}Tl (range 3.6–7.3) in each of the six dual-isotope sestamibi ^{201}Tl hearts. Although this difference was statistically significant in the paired dual-isotope comparisons, there was no significant difference in the mean contrast values from the unpaired single-isotope sestamibi and ^{201}Tl hearts in the presence of a relatively large standard deviation (Table 2).

Hypoperfusion produced by coronary occlusion resulted in autoradiographic defects from sestamibi that were not significantly different from simultaneously injected ^{201}Tl (Table 3).

Teboroxime Versus Sestamibi

Teboroxime defects appeared more sharply delineated than sestamibi defects. Comparison of the measured normal-to-defect contrast between the two ^{99m}Tc-based agents was necessarily confined to the single-isotope hearts, as seen in Table 2. In these groups, the mean contrast on teboroxime autoradiographs exceeded that of sestamibi (22.2 ± 7.4 versus 10.0 ± 3.0).

Control Measurements

Profile lines across ^{99m}Tc and ^{201}Tl standard discs were compared to exclude an inherent difference in the two isotopes in demonstrating a border. These ^{99m}Tc and ^{201}Tl profiles were virtually indistinguishable (Fig. 7).

Defects were not seen in the sham-operated rabbits. The observed homogeneity of ^{201}Tl and teboroxime distribution was confirmed by profile lines that always showed <5% variation in tracer activity.

DISCUSSION

On the basis of tracer content, the ^{99m}Tc-based myocardial perfusion agents, teboroxime and, to a lesser extent, sestamibi, produced sharper transition zones and better normal-to-low flow contrast than simultaneously administered ^{201}Tl. The ^{99m}Tc agents were better able to differentiate normal and hypoperfused myocardium. The sharper transition zone and higher contrast of teboroxime images resulted in measurement of larger defects than ^{201}Tl. Autoradiographs from the dual sestamibi and ^{201}Tl hearts did not show a significant difference in defect size.

Quality Control

These findings cannot be attributed to the inherent imaging properties of ^{99m}Tc and ^{201}Tl because tracer profiles produced from ^{99m}Tc and ^{201}Tl standard discs were indistinguishable. The results were not likely to have been influenced by dual-isotope separation or by the effect of one isotope on uptake and retention of the other isotope, because similar values were obtained from the single- and the dual-isotope experiments. Enhanced ^{99m}Tc contrast cannot be attributed to injected 300-fold ^{99m}Tc/^{201}Tl excess because the dose delivered to each film by ^{99m}Tc was matched to that of ^{201}Tl by the appropriate selection of exposure times (Fig. 1). Tracer activities for ^{201}Tl and ^{99m}Tc were extrapolated from the same part of their respective standard curves.

When ^{201}Tl was coinjected with teboroxime, the circulation time was limited to 2 min to preclude rapid redistribution of teboroxime (*23*). Difference in circulation time

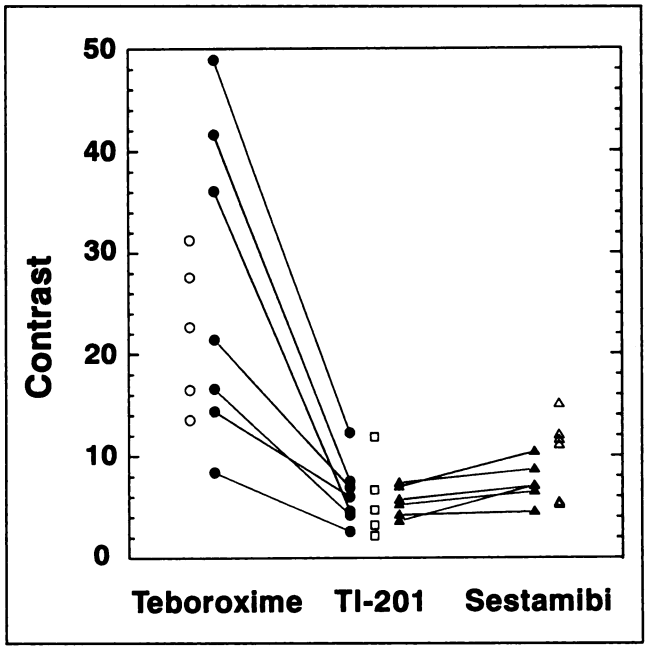

FIGURE 4. Plots of normal-to-defect activity ratios for single-isotope teboroxime (○), sestamibi (△) and Tl-201 (□) and dual-isotope teboroxime/^{201}Tl (●–●) and sestamibi/^{201}Tl (▲–▲) hearts.

TABLE 2
Normal-to-Defect Activity Contrast Produced by Teboroxime, Sestamibi and ^{201}Tl

Rabbit	Teboroxime*	^{201}Tl	Rabbit	Sestamibi†	^{201}Tl
Dual Isotope					
1	16.6	4.2	8	6.5	5.2
2	14.4	6.0	9	7.1	3.6
3	8.4	2.6	10	8.6	7.3
4	36.1	4.6	11	4.5	4.3
5	41.6	7.5	12	10.4	7.0
6	48.9	12.3	13	7.0	5.7
7	21.4	6.9			
Mean	26.8	6.3		7.3	5.5
s.d.	(15.4)	(3.1)		(2.0)	(1.5)

Rabbit	Teboroxime‡	Rabbit	^{201}Tl§	Rabbit	Sestamibi
Single Isotope					
14	13.6	19	2.1	24	5.2
15	16.5	20	3.2	25	5.4
16	22.7	21	4.7	26	11.0
17	27.6	22	6.7	27	11.5
18	31.3	23	11.9	28	12.0
				29	15.0
Mean	22.3		5.7		10.0
s.d.	(7.4)		(3.8)		(3.0)

*$p < 0.02$ for teboroxime versus ^{201}Tl.
†$p < 0.03$ for sestamibi versus ^{201}Tl.
‡$p < 0.001$ for teboroxime versus ^{201}Tl; $p < 0.007$ for teboroxime versus sestamibi.
§p = NS for ^{201}Tl versus sestamibi.

for ^{201}Tl in this group (versus 5 min in the ^{201}Tl sestamibi and single-isotope ^{201}Tl groups) would not be expected to significantly affect retention of this tracer. Recent studies have shown that retention of ^{201}Tl (and sestamibi) does not vary between 2 and 5 min (*26*). Moreover, normal-to-defect contrast for ^{201}Tl was independent of circulation time (Table 2).

Interspecies variability in tracer kinetics warrants caution when extrapolating results of animal studies to clinical scintigraphy. However, results based on the present rabbit model have correlated well with clinical data for ^{201}Tl, sestamibi and teboroxime (*27–29*).

TABLE 3
Percent Defect Area Delineated by Teboroxime, Sestamibi and ^{201}Tl in Dual-Isotope Hearts

Rabbit	Teboroxime*	^{201}Tl	Rabbit	Sestamibi†	^{201}Tl
1	10.5	9.1	8	24.1	25.6
2	25.7	25.3	9	10.5	12.2
3	16.6	12.4	10	42.6	40.4
4	12.9	10.4	11	3.1	7.5
5	12.7	11.2	12	31.5	34.3
6	12.5	10.6	13	9.8	11.2
7	21.2	11.8			
Mean	16.0	12.9		20.3	21.9
s.d.	(5.6)	(5.3)		(15.1)	(13.6)

*$p < 0.02$ for teboroxime versus ^{201}Tl.
†p = NS for sestamibi versus ^{201}Tl.

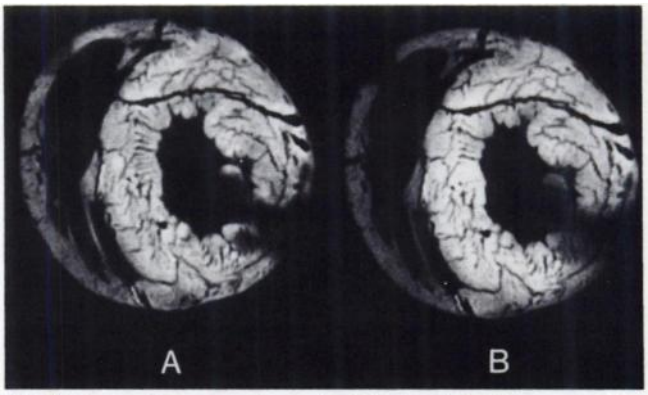

FIGURE 5. Representative pair of digitized dual-isotope activity autoradiographs showing ^{99m}Tc sestamibi (A) and ^{201}Tl (B) activity distributions in the same heart. Note the increased contrast and clearer delineation of normal and low flow zones produced by sestamibi compared to simultaneously injected ^{201}Tl.

Differences in Tracer Distribution

Uptake of the three tracers results from a complex interaction of hemodynamic and metabolic factors. While teboroxime has a more direct proportional increase in net extraction with higher blood flow than either sestamibi or ^{201}Tl in the isolated perfused rabbit heart model (*30*), kinetics of initial tracer transport may not fully explain observed differences in contrast (*31*). Myocardial tracer uptake is believed to predominantly reflect coronary blood flow (*4,13–16,27,32–34*). However, myocardial uptake of ^{201}Tl and cellular retention of sestamibi appear to involve active cellular processes and thus may be affected by the myocyte metabolic state. A metabolic role in uptake and cellular retention of ^{201}Tl and sestamibi has been suggested from both clinical and basic studies (*2,31,35–37*). This property has led to clinical inference and subsequent evaluation of cell viability on the basis of ^{201}Tl or sestamibi

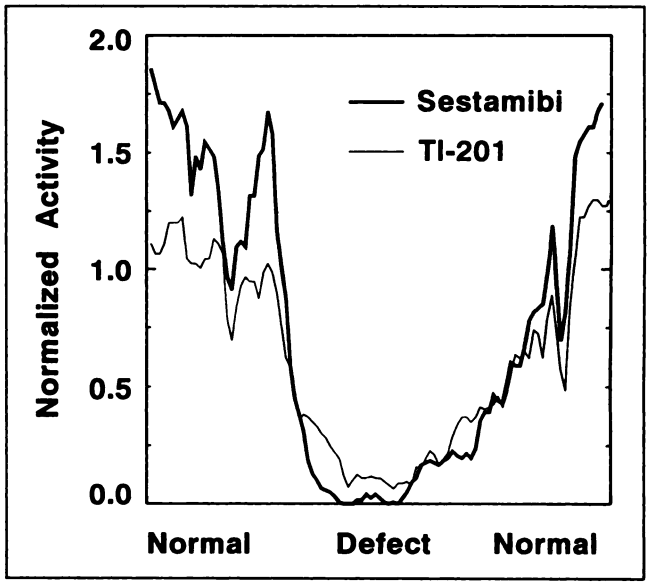

FIGURE 6. Representative pair of dual-isotope ^{99m}Tc sestamibi/^{201}Tl profiles across a defect showing an increased normal-to-defect contrast and a sharper normal-to-defect transition for sestamibi compared to simultaneously injected ^{201}Tl.

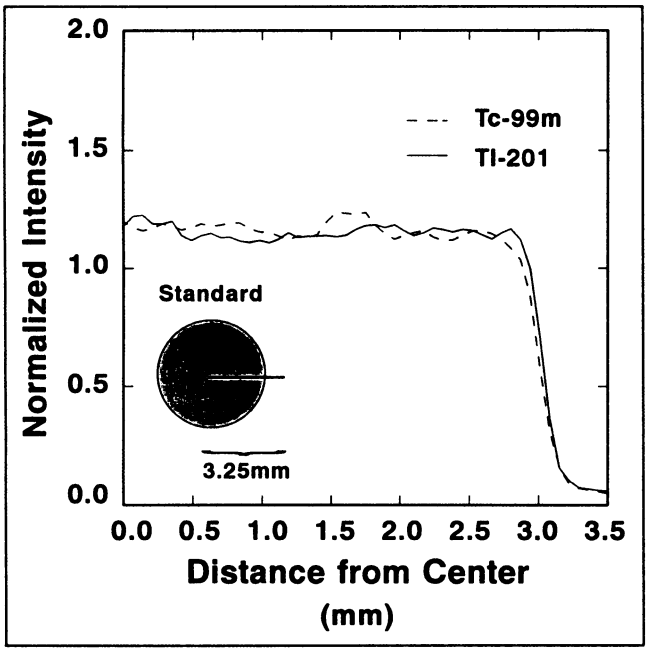

FIGURE 7. Intensity profiles across ^{201}Tl and ^{99m}Tc standard discs, showing no inherent difference in sensitivity between the two isotopes in delineating a border.

uptake (*6,38–42*). While a metabolic effect on teboroxime uptake has been observed (*36,43*), recent studies have shown that uptake of this tracer is less sensitive to metabolic insult than either sestamibi or ^{201}Tl in cultured myocytes (*44*), and is independent of viability in the intact rabbit heart (*45*).

In our basic model, differences in tracer uptake may be expected to relate predominantly to flow. However, while 5 min of total coronary occlusion is insufficient to cause substantial myocardial necrosis in rabbits (*46*), this insult is associated with significant ischemia and concomitant metabolic abnormalities. A degree of metabolic and hemodynamic alterations would be expected to occur in clinical imaging of acute ischemic episodes. Therefore, the metabolic abnormalities created in this model would strengthen its clinical correlation.

We would expect all three agents to show a good linear correlation at normal physiological blood flow levels (*29,31,47*). However, as flow is greatly diminished, peak extraction of ^{201}Tl, sestamibi and, to a lesser extent, teboroxime, tends to increase, suggesting that teboroxime may provide "enhanced" contrast between normal and low flow zones. Experimental evidence for this is the fact that ^{201}Tl and sestamibi uptake is disproportionately higher than expected in comparison to microsphere-determined blood flow at the levels of less than 0.4 ml/min/g that are typically associated with acute coronary occlusions (*12,13,32,48,49*). In the type of studies associated with acute coronary occlusions, tracer uptake has consistently exceeded microsphere-based flow. Previous work has shown that myocardial uptake of teboroxime is more linear than sestamibi or ^{201}Tl at both high and low flow ranges (*29,31,33*). Increased normal-to-defect contrast of teboroxime suggests that it does not overestimate flow at low levels and may therefore more accurately reflect the true range of myocardial blood flow than either ^{201}Tl or sestamibi.

The possibility that ^{99m}Tc compounds amplify contrast compared to ^{201}Tl is not supported by previous work, which uniformly demonstrates that regional tracer uptake does not overestimate flow disparities (*6,7,12–15,29,31, 33,48,49*).

Teboroxime demonstrated the most discrete transition zone between normal and hypoperfused zones. The question of which tracer most accurately delineates the actual transition in blood flow is beyond the resolution attainable with standard microsphere techniques. However, Alden et al. (*50*), using a high-resolution fluorophotometric method, studied the transition between the perfused and ischemic zones in rabbit myocardium distal to a coronary occlusion. They concluded that the transition distance from control levels of coronary blood flow to <1% of control is approximately 50 μm or less. This supports the conclusion that teboroxime more accurately delineates a border than either sestamibi or ^{201}Tl.

This study assessed ability of the three tracers to detect hypoperfusion within the range not exceeding normal, which has previously been determined to be approximately 0.68 ml/g/min (*51*). Coronary hyperemia was not induced pharmacologically so we cannot extrapolate our conclusions to disparities in the hyperemic coronary blood flow obtained in exercise or dipyridamole stress testing. Based on the isolated perfused heart and other models, ^{201}Tl and sestamibi maintain linear myocardial uptake with coronary blood flows up to 2.5–3 ml/min/g (*29*) with teboroxime having a greater range of linear uptake (>4 ml/min/g) (*33*). In preliminary work in hyperemic swine, teboroxime produced greater normal-to-defect contrast compared to ^{201}Tl (*52*). Therefore, it is likely that similar results would be obtained in the presence of coronary hyperemia.

Differences In Defect Size

Defect size was assessed visually by delineating regions of low intensity on the autoradiographs. Heterogeneity in vascular distribution resulted in a high degree of interrabbit variability in the area of hypoperfusion produced by coronary occlusion. This variation would be expected to obscure any differences in defect size when the three tracers are compared in separate groups of single-isotope autoradiographs. Since all three tracers cannot be coinjected into one heart, we limited the analysis of defect size to paired dual-isotope comparisons of teboroxime versus ^{201}Tl and sestamibi versus ^{201}Tl. The sharper transition and higher contrast of teboroxime compared to ^{201}Tl resulted in larger autoradiographic defects displayed by teboroxime. This implies that teboroxime more accurately reflects the extent of hypoperfused myocardium than the other tracers. While the size of sestamibi and ^{201}Tl defects did not differ when analyzed by dual-isotope comparison, ^{201}Tl defects derived from dual-sestamibi/^{201}Tl hearts were much larger than

those derived from the dual-teboroxime/^{201}Tl hearts (Table 3). This difference in ^{201}Tl defect size in the two dual-isotope groups is probably a chance occurrence stemming from high variability between rabbits. Thus, only dual-isotope analysis between ^{99m}Tc agents and ^{201}Tl is meaningful in comparison of defect size.

Limitations of the Study

An apparent limitation of this study is the absence of corresponding blood flow data. Thus, one cannot be certain that the enhanced contrast of teboroxime and sestamibi accurately reflect "true" contrast in myocardial blood flow. This method allocates most of the myocardium to preparation of quantitative autoradiographs and therefore is not compatible with segmental myocardial microsphere determination. However, resolution of autoradiography exceeds that achievable with segmental microsphere counting and is a better technique to assess regional gradients in coronary flow.

We evaluated the initial tracer deposition within the time interval applied routinely between tracer administration and clinical imaging. Accordingly, washout data was not obtained.

Advantages of the Method

This method of radioisotope analysis produces high-resolution images of isolated, ultra-thin myocardial slices. Film intensity is exponentially related to tracer activity and this relationship varies with each film and development process (*25*). Therefore, use of intensity on autoradiographs is limited to cursory nonquantitative evaluation of tracer content. The method described here produces actual tracer activity images and allows tracer activity to be determined at any point in the activity image. Two or more isotopes that differ in half-life or potentially by emitted energy can be studied simultaneously, with judiciously chosen injected doses or appropriate shielding. Thus, this analysis provides a basis for applying these methods to a broad range of cardiac research.

Clinical Implications and Conclusions

The assessment of area at risk in experimental models pertains to clinical questions and suggests appropriate imaging protocols based on tracer properties. While myocardial kinetics, target-to-background uptake and ease of use determine how and in what clinical settings they are used, the diagnostic accuracy of myocardial perfusion tracers is ultimately based on their ability to reflect flow disparities.

Teboroxime and, to a lesser extent, sestamibi, produce superior uptake contrast to ^{201}Tl between normal and hypoperfused rabbit myocardium and would therefore be expected to yield greater diagnostic accuracy for the presence and extent of hypoperfused myocardium in appropriate clinical situations. This study is applicable, but not limited to, diagnostic settings such as the detection of ischemia at rest, the evaluation of the area at risk in acute myocardial infarction or other indications in which a resting injection may be used to detect disparities in tracer uptake. Teboroxime and sestamibi are particularly well suited for these indications because of rapid (5 min) serial imaging potential of teboroxime and the image stability of sestamibi that allows for the "uncoupling" of clinical imaging from tracer injection. Initial clinical studies exploiting these properties have been promising (*8–11*). In clinical imaging, ^{201}Tl emissions are scattered to a greater extent than ^{99m}Tc, which would further accentuate the difference in contrast between ^{99m}Tc-based agents and ^{201}Tl. Sestamibi images have been reported to be "crisper" than their ^{201}Tl counterparts (*5*), and diagnostic accuracy of both sestamibi and teboroxime has been confirmed in clinical studies (*5,53–57*).

Based on quantitative dual-isotope autoradiography, we conclude that teboroxime, and to a lesser extent, sestamibi, can better delineate hypoperfused myocardium when compared to ^{201}Tl. Teboroxime detects the largest area of hypoperfusion and may provide the most accurate assessment of myocardium-at-risk distal to coronary stenosis.

ACKNOWLEDGMENTS

The authors thank Drs. Seth Dahlberg and Bernard Villegas for their useful discussions; John Wironen and Robert Siwko for technical assistance, and Harriet Kay for help in preparing the manuscript. We also wish to acknowledge the product support and encouragement from Dr. William Eckelman (Bristol Myers Squibb) and Dr. Martin Thoolin (Du Pont Pharma). This manuscript was supported in part by National Institutes of Health Research Grant RO1 HL 34199 and American Heart Association Grant-in-Aid 89-978.

REFERENCES

1. Narra RK, Nunn AD, Kuczynski BL, et al. A neutral technetium-99m complex for myocardial imaging. *J Nucl Med* 1989;30:1830–1837.
2. Maublant JC, Moins N, Gachon P. Uptake and release of two new ^{99m}Tc-labeled myocardial blood flow imaging agents in cultured cardiac cells. *Eur J Nucl Med* 1989;15:180–182.
3. Stewart RE, Schwaiger M, Hutchins GD, et al. Myocardial clearance kinetics of technetium-99m-SQ30217: a marker of regional myocardial blood flow. *J Nucl Med* 1990;31:1183–1190.
4. Okada RD, Glover D, Gaffney T, Williams S. Myocardial kinetics of technetium-99m-hexakis-2-methoxy-2-methylpropyl-isonitrile. *Circulation* 1988; 77:491–498.
5. Wackers FJTh, Berman DS, Maddahi J, et al. Technetium-99m hexakis 2-methoxy-isobutyl isonitrile: human biodistribution, dosimetry, safety and preliminary comparison to thallium-201 for myocardial perfusion imaging. *J Nucl Med* 1989;30:301–311.
6. Okada RD. Kinetics of thallium-201 in reperfused canine myocardium after coronary artery occlusion. *J Am Coll Cardiol* 1984;3:1245–1251.
7. Grunwald AM, Watson DD, Holzgrefe HH Jr, Irving JF, Beller GA. Myocardial thallium-201 kinetics in normal and ischemic mocardium. *Circulation* 1981;64:610–618.
8. Heller LI, Weiner BH, Dahlberg ST, et al. Rapid sequential teboroxime imaging for the detection of successful coronary reperfusion [Abstract]. *Circulation* 1991;84:II-302.
9. Gibbons RJ, Verani MS, Behrenbeck T, et al. Feasibility of tomographic ^{99m}Tc-hexakis-2-methoxy-2-methylpropylisonitrile imaging for the assessment of myocardial area at risk and the effect of treatment in acute myocardial infarction. *Circulation* 1989;80:1277–1286.
10. Bilodeau L, Théroux P, Grégoire J, Gagnon D, Arsenault A. Technetium-99m sestamibi tomography in patients with spontaneous chest pain: correlations with clinical, electrocardiographic and angiographic findings. *J Am Coll Cardiol* 1991;18:1684–1691.
11. Becker LC. Technetium-99m sestamibi tomography in patients with spontaneous chest pain. *J Am Coll Cardiol* 1991;18:1692–1693.

12. Sinusas AJ, Watson DD, Cannon JM Jr, Beller GA. Effect of ischemia and postischemic dysfunction on myocardial uptake of technetium-99m-labeled methoxyisobutyl isonitrile and thallium-201. *J Am Coll Cardiol* 1989;14: 1785–1793.
13. Li Q-S, Frank TL, Franceschi D, Wagner HN Jr, Becker LC. Technetium-99m methoxyisobutyl isonitrile (RP30) for quantification of myocardial ischemia and reperfusion in dogs. *J Nucl Med* 1988;29:1539–1548.
14. Mousa SA, Cooney JM, Williams SJ. Relationship between regional myocardial blood flow and the distribution of ^{99m}Tc-sestamibi in the presence of total coronary artery occlusion. *Am Heart J* 1990;119:842–847.
15. Gray WA, Gewirtz H. Comparison of ^{99m}Tc-teboroxime with thallium for myocardial imaging in the presence of a coronary artery stenosis. *Circulation* 1991;84:1796–1807.
16. Strauss HW, Harrison K, Langan JK, Lebowitz E, Pitt B. Thallium-201 for myocardial imaging: relation of thallium-201 to regional myocardial perfusion. *Circulation* 1975;51:641–645.
17. DeBoer LWV, Strauss HW, Kloner RA, et al. Autoradiographic method for measuring the ischemic myocardium at risk: effects of verapamil on infarct size after experimental coronary artery occlusion. *Proc Natl Acad Sci USA* 1980;77:6119–6123.
18. Khaw BA, Fallon JT, Beller GA, Haber E. Specificity of localization of myosin-specific antibody fragments in experimental myocardial infarction: histologic, histochemical, autoradiographic and scintigraphic studies. *Circulation* 1979;60:1527–1531.
19. Dae MW, Velazquez-Rocha SJ, Botvinick EH, O'Connell JW. Comparison of thallium and Tc-sestamibi in isoproterenol induced subendocardial ischemia in rat myocardium [Abstract]. *J Am Coll Cardiol* 1992;19:337A.
20. Di Rocco RJ, Bauer A, Pirro JP, et al. Regional myocardial metabolism, blood flow and misonidazole retention after occlusion of the left anterior descending coronary artery in rabbits [Abstract]. *J Nucl Med* 1992;33:993.
21. Dae M, Velazquez Rocha S, Wolfe C, Botvinick E, O'Connell W. High resolution scintigraphic assessment of thallium and Tc-MIBI in ischemic and reperfused rat hearts [Abstract]. *J Am Coll Cardiol* 1991;17:287A.
22. Lurie KG, Dae MW, Rocha S, et al. Metaiodobenzylguanidine as an index of AV nodal adrenergic activity [Abstract]. *Circulation* 1990;82:III-455.
23. Weinstein H, Dahlberg ST, McSherry BA, Hendel RC, Leppo JA. Rapid redistribution of teboroxime. *Am J Cardiol* 1993;71:848–852.
24. Ito T, Brill AB. Validity of tissue paste standards for quantitative whole-body autoradiography using short-lived radionuclides. *Appl Radiat Isot* 1990;41:661–667.
25. Johns HE, Cunningham JR. Diagnostic radiology. In: *The physics of radiology*. 4th ed. Springfield, IL: Charles C. Thomas; 1983:557–669.
26. Melon PG, Beanlands RS, DeGrado TR, et al. Comparison of technetium-99m sestamibi and thallium-201 retention characteristics in canine myocardium. *J Am Coll Cardiol* 1992;20:1277–1283.
27. Leppo JA, MacNeil PB, Moring AF, Apstein CS. Separate effects of ischemia, hypoxia and contractility on thallium-201 kinetics in rabbit myocardium. *J Nucl Med* 1986;27:66–74.
28. Marshall RC, Leidholdt EM Jr, Zhang D-Y, Barnett CA. Technetium-99m hexakis 2-methoxy-2-isobutyl isonitrile and thallium-201 extraction, washout and retention at varying coronary flow rates in rabbit heart. *Circulation* 1990;82:998–1007.
29. Leppo JA, Meerdink DJ. Comparative myocardial extraction of two technetium-labeled BATO derivatives (SQ30217, SQ32014) and thallium. *J Nucl Med* 1990;31:67–74.
30. Meerdink DJ, Leppo JA. Evaluation of perfusion imaging tracer "uptake" by net extraction*flow vs flow plots [Abstract]. *Circulation* 1990;82:III-487.
31. Meerdink DJ, Leppo JA. Experimental studies of the physiologic properties of technetium-99m agents: myocardial transport of perfusion imaging agents. *Am J Cardiol* 1990;66:9E–15E.
32. Melin JA, Becker LC, Bulkley BH. Differences in thallium-201 uptake in reperfused and nonreperfused myocardial infarction. *Circ Res* 1983;53:414–419.
33. DiRocco RJ, Rumsey WL, Kuczynski BL, et al. Measurement of myocardial blood flow using a co-injection technique for technetium-99m-teboroxime, technetium-96-sestamibi and thallium-201. *J Nucl Med* 1992;33:1152–1159.
34. Beller GA, Watson DD. Physiological basis of myocardial perfusion imaging with the technetium-99m agents. *Semin Nucl Med* 1991;21:173–181.
35. Maublant JC, Gachon P, Moins N. Hexakis (2-methoxy isobutylisonitrile) technetium-99m and thallium-201 chloride: uptake and release in cultured myocardial cells. *J Nucl Med* 1988;29:48–54.
36. Johnson G, Moffett JD, Hebert CB, Okada RD. Myocardial Tc-99m-teboroxime (CardioTec) clearance is affected by myocardial metabolic status and myocyte membrane integrity [Abstract]. *J Am Coll Cardiol* 1992;19: 338A.
37. Okada RD, Johnson G, Glover DK, Hebert CB. Myocardial Tc-99m-teboroxime (Cardiotec, SQ30217) clearance is reduced in ischemic myocardium due to a combination of hypoxic and low flow factors [Abstract]. *J Am Coll Cardiol* 1991;17:286A.
38. Dilsizian V, Freedman NMT, Bacharach SL, Perrone-Filardi P, Bonow RO. Regional thallium uptake in irreversible defects: magnitude of change in thallium activity after reinjection distinguishes viable from nonviable myocardium. *Circulation* 1992;85:627–634.
39. Kayden DS, Sigal S, Soufer R, et al. Thallium-201 for assessment of myocardial viability: quantitative comparison of 24-hr redistribution imaging with imaging after reinjection at rest. *J Am Coll Cardiol* 1991;18:1480–1486.
40. Cuocolo A, Pace L, Ricciardelli B, Chiarello M, Trimarco B, et al. Identification of viable myocardium in patients with chronic coronary artery disease: comparison of thallium-201 scintigraphy with reinjection and technetium-99m-methoxyisobutyl isonitrile. *J Nucl Med* 1992;33:505–511.
41. Freeman I, Grunwald AM, Hoory S, Bodenheimer MM. Effect of coronary occlusion and myocardial viability on myocardial activity of technetium-99m-sestamibi. *J Nucl Med* 1991;32:292–298.
42. Piwnica-Worms D, Chiu ML, Kronauge JF. Divergent kinetics of ^{201}Tl and ^{99m}Tc-Sestamibi in cultured chick ventricular myocytes during ATP depletion. *Circulation* 1992;85:1531–1541.
43. Chang PI, Shi Q-X, Maniawski P, et al. Tc-99m-teboroxime is a marker of reperfusion flow early after acute myocardial infarction [Abstract]. *J Am Coll Cardiol* 1992;19:338A.
44. Maublant JC, Moins N, Gachon P, et al. Uptake of technetium-99m-teboroxime in cultured myocardial cells: comparison with thallium-201 and technetium-99m-sestamibi. *J Nucl Med* 1993;34:255–259.
45. Villegas BJ, Heller LI, Reinhardt CP, et al. Teboroxime as a marker of reperfusion during acute myocardial infarction independent of myocardial viability [Abstract]. *J Am Coll Cardiol* 1993;21:376A.
46. Connelly CM, Vogel WM, Hernandez YM, Apstein CS. Movement of necrotic wavefront after coronary occlusion in rabbit. *Am J Physiol* 1982; 243:H682–H690.
47. Leppo JA, DePuey EG, Johnson LL. A review of cardiac imaging with sestamibi and teboroxime. *J Nucl Med* 1991;32:2012–2022.
48. De Coster PM, Wijns W, Cauwe F, et al. Area-at-risk determination by technetium-99m-hexakis-2-methoxyisobutyl isonitrile in experimental reperfused myocardial infarction. *Circulation* 1990;82:2152–2162.
49. Sinusas AJ, Trautman KA, Bergin JD, et al. Quantification of area at risk during coronary occlusion and degree of myocardial salvage after reperfusion with technetium-99m methoxyisobutyl nitrile. *Circulation* 1990;82: 1414–1437.
50. Harken AH, Simson MB, Haselgrove J, et al. Early ischemia after complete coronary ligation in the rabbit, dog, pig and monkey. *Am J Physiol* 1981; 241:H202–H210.
51. Bassingthwaighte JB, Malone MA, Moffett TC, et al. Validity of microsphere depositions for regional myocardial flows. *Am J Physiol* 1987;253: H184–H193.
52. Berman SF, Gray WA, Gewirtz H. Comparison of technetium-99m-teboroxime and thallium for assessment of relative coronary flow reserve in the presence of coronary artery stenosis [Abstract]. *J Am Coll Cardiol* 1992;19:338A.
53. Taillefer R, Lambert R, Essiambre R, Phaneuf DC, Leveille J. Comparison between thallium-201, technetium-99m-sestamibi and technetium-99m-teboroxime planar myocardial perfusion imaging in detection of coronary artery disease. *J Nucl Med* 1992;33:1091–1098.
54. Johnson LL. Clinical experience with technetium-99m teboroxime. *Semin Nucl Med* 1991;21:182–189.
55. Labonte C, Taillefer R, Lambert R, et al. Comparison between technetium-99m-teboroxime and thallium-201 dipyridamole planar myocardial perfusion imaging in detection of coronary artery disease. *Am J Cardiol* 1992;69:90–96.
56. Seldin DW, Johnson LL, Blood DK, et al. Myocardial perfusion imaging with technetium-99m SQ30217: comparison with thallium-201 and coronary anatomy. *J Nucl Med* 1989;30:312–319.
57. Dahlberg ST, Weinstein H, Hendel RC, McSherry B, Leppo JA. Planar myocardial perfusion imaging with technetium-99m-teboroxime: comparison by vascular territory with thallium-201 and coronary angiography. *J Nucl Med* 1992;33:1783–1788.